https://doi.org/10.31871/WJIR.17.5.3
World Journal of Innovative Research (WJIR)
ISSN: 2454-8236, Volume-17, Issue-5, November 2024 Pages 01-18

Transthoracic Echocardiography: Estimation of Mitral Annulus Disjunction And LV Strain Parameters In Mitral Valve Prolapse - A Singular Case Report And Literature Review

Akhil Mehrotra , Mohammad Shaban , Faiz Illahi Siddiqui

***Abstract*— Mitral valve prolapse (MVP) is usually asymptomatic, but can be associated with complications such as infective endocarditis, mitral regurgitation, thromboembolism and sudden cardiac death. Myxomatous degeneration is the most common cause of MVP and it can be associated with involvement of the other valves.**

Mitral annular disjunction (MAD) is an associated abnormality where a portion of the mitral valve annulus attaches superiorly in the left atrial wall. This abnormal displacement may lead to fibrosis in the region of the disjunction and may serve as a nidus for arrhythmias. The association between MVP with MAD and its predisposition to ventricular arrhythmias (VAs) such as ventricular fibrillation (VF), ventricular tachycardia (VT), and premature ventricular contraction (PVCs) has been reported in multiple studies and case reports. While MAD is increasingly recognized, its clinical significance, especially in association with MVP, remains an area of active investigation.

It is very well known that MVP may lead to mitral valve regurgitation which may increase over time and cause moderate to severe mitral regurgitation with the development left ventricular (LV) systolic dysfunction in later stages. 2-Dimensional speckle tracking echocardiography has been utilized for more than two decades to detect LV systolic dysfunction by LV strain imaging, which may pick up the LV aberrations priorto its presentation on routine 2-Dimensional echocardiography.

We present here a case of 54 year Indian male presenting with MVP accompanied by significant mitral annulus disjunction (MAD) in whom a comprehensive transthoracic echocardiography (TTE) and 4Dimensional XStrain speckle tracking imaging was conducted to estimate the MAD distance and importantly, various LV strain parameters were evaluated. Perhaps this is the first case report of impact of MVP and MAD on LV deformation parameters evaluated by 4Dimensional XStrain speckle tracking echocardiography (STE).

***Index Terms*— mitral valve prolapse (MVP), mitral annulus disjunction, MAD, mitral regurgitation, mitral valve anatomy, LV strain imaging in MVP, 4Dimensional XStrain echocardiography in MAD..**

Akhil Mehrotra , Chief, Pediatric and Adult Cardiology, Prakash Heart Station, Nirala Nagar, Lucknow, UP, India.
Mohammad Shaban , Cardiac Technician, Prakash Heart Station, Nirala Nagar, Lucknow, UP, India.
Faiz Illahi Siddiqui, Cardiac Technician, Prakash Heart Station, Nirala Nagar, Lucknow, UP, India.

I. INTRODUCTION

Highlight Mitral valve prolapse (MVP), also known as floppy mitral valve syndrome, systolic click-murmur syndrome, and billowing mitral leaflets, is a valvular heart disease disorder (Figure 1).

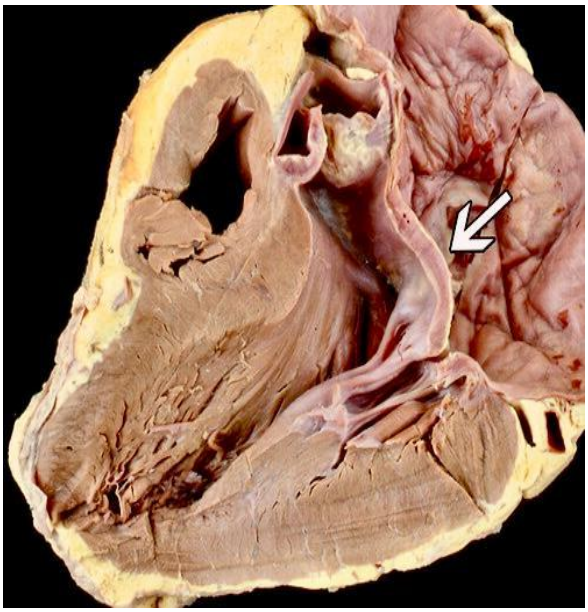

Figure 1: Pathological specimen of MVP. Arrow denotes anterior mitral valve prolapse

It is a benign condition. In rare cases, it may present with sudden cardiac death, endocarditis, or a stroke [1-3]. The condition affects nearly 3% of the United States population. The disorder produces symptoms due to a redundant and abnormally thickened mitral valve leaflet prolapsing into the left atrium during systole. MVP is usually identified during a clinical exam on cardiac auscultation. Echocardiography confirms the diagnosis (Figure 2). This disorder is the most common cause of the non-ischemic mitral regurgitation in the US [4]. Symptomatic patients may need mitral valve repair.

(A)

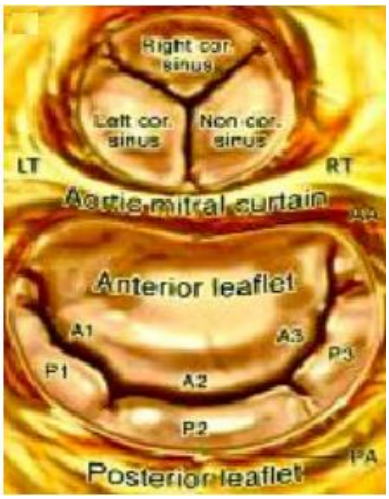

(B)

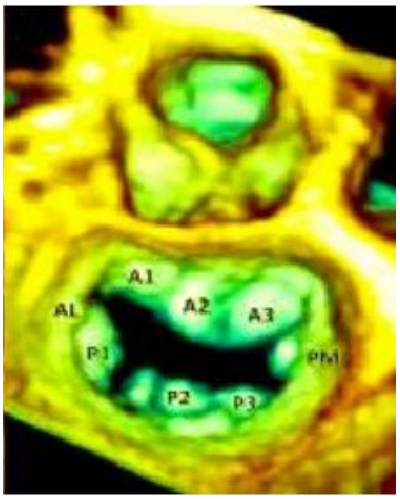

(C)

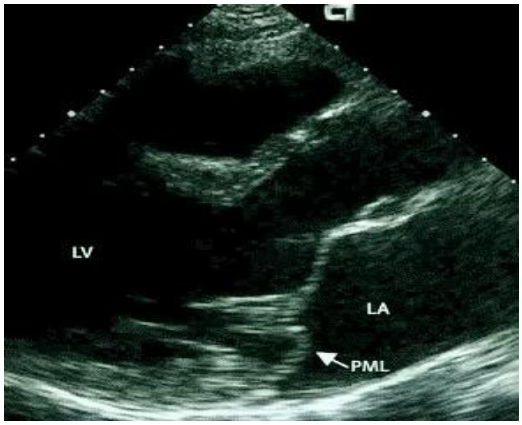

(D)

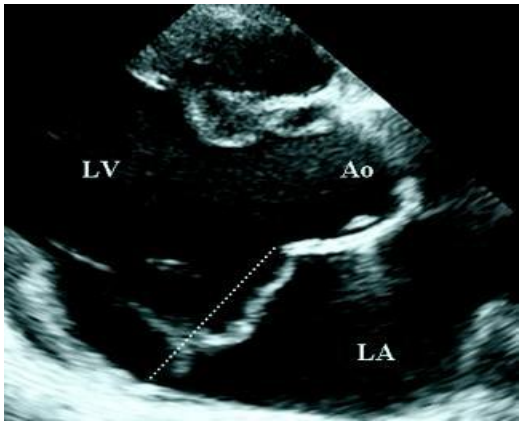

(E)

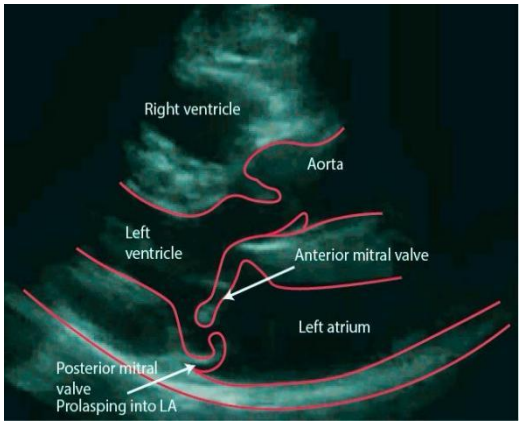

(F)

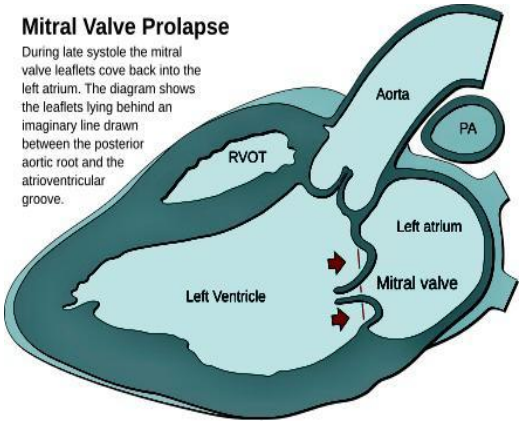

Figure 2: (A) Normal mitral valve anatomy showing anterior and posterior leaflets and annuluses. The anterior annulus is separated from the aortic root by the fibrous intertrigonal region, also known as the aortic-mitral curtain, which is surrounded by the right and left fibrous trigones. (B) 3D Transesophageal echocardiography (TEE) image from surgeon's view of normal mitral valve anatomy as described above. LT = left trigone, RT = right trigone, AA = anterior annulus, PA = posterior annulus, AL = anterolateral commissure, PM = posteromedial commissure. (C) Classic 2Dimensional transthoracic view for detection of mitral valve prolapse; (D) Mitral annular line is depicted as a dotted line. The amount of superior displacement of anterior and posterior mitral valve leaflets are measured; (E) and (F) Diagrammatic illustration of MVP

Definition of mitral valve prolapse

In a Framingham Heart Study, Freed et al historically described echocardiographic criteria for MVP as classic versus nonclassic [5]. It is of paramount importance to view and diagnose MVP in the parasternal long axis view [6], and not in any other views. This is due to the reason that imaging in this view reduces the over diagnosis of MVP [6].

Echocardiographic findings/diagnostic criteria for MVP are as follows [5] (Figure 3, Table 1):

- Classic MVP: The parasternal long-axis view shows more than 2 mm superior displacement of the mitral leaflets into the left atrium during systole, with a leaflet thickness of at least 5 mm.
- Nonclassic MVP: Displacement is more than 2 mm, with a maximal leaflet thickness below 5 mm.
- Other: Other echocardiographic findings that should be considered as criteria are leaflet thickening, redundancy, annular dilatation, and chordal elongation.

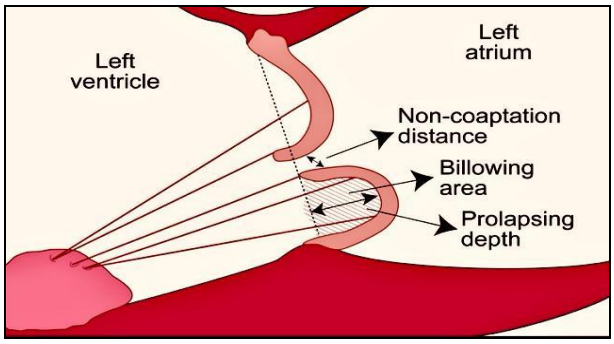

(A) Illustration of multiple features of MVP (non- coaptation distance, billowing area and prolapsing depth)

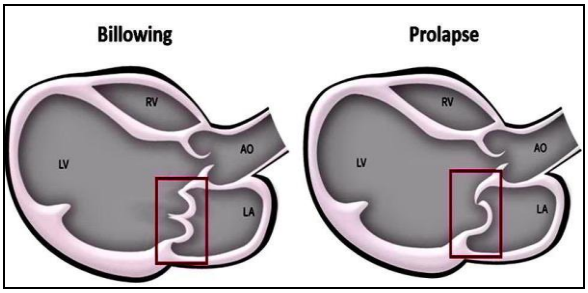

(B) Leaflet body displaced into LA, Leaflet tips stay at annular level or above into LV and Leaflet tips displaced into LA from annular plane

Figure 3: Diagrammatic illustration of the criteria for the diagnosis of MVP

Table 1: Tabular depiction of mitral valve prolapse criteria

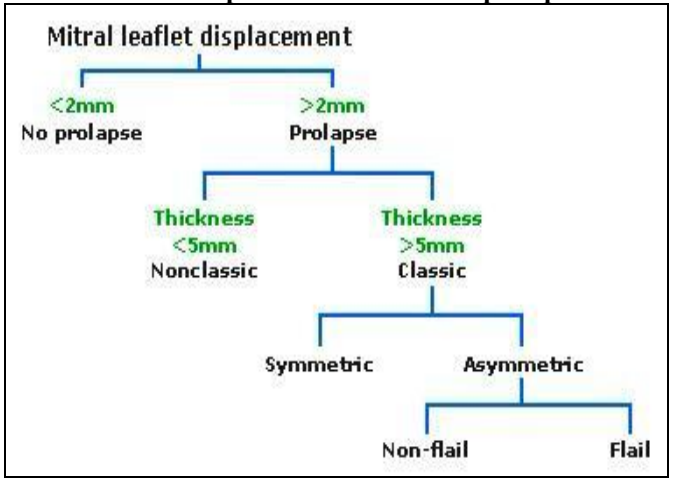

Mitral annular disjunction

Recently, the presence and severity of mitral annular disjunction (MAD), the potential mechanism responsible for ventricular arrhythmias (VAs),have been studied intensively [7-9] (Figure 4).

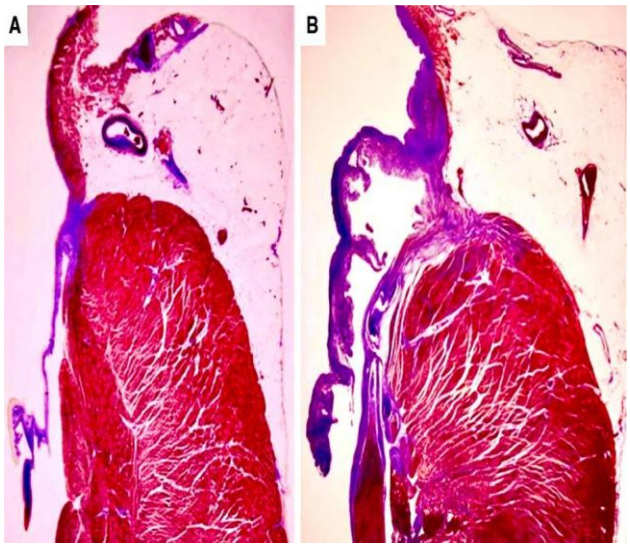

Figure 4: Morphological histology of mitral valve annulus, delineating. (A) Mitral annulus with MV insertion in a normal healthy heart; (B) a heart with MAD. The staining allowed identification of muscle (red) and collagen (blue). MAD is diagnosed on the separation of between posterior MV leaflet insertion into the thinner LA tissue and the junction of LA to the thicker muscular LV tissue. A greater degree of fibrosis, indicated by the blue-stained collagenous tissue, is identified in heart with MAD.

MAD is an abnormal systolic displacement of the hinge point of the mitral valve away from the LV myocardium wall [10], most frequently localized under the posterior mitral valve leaflet[10] (Figure 5).

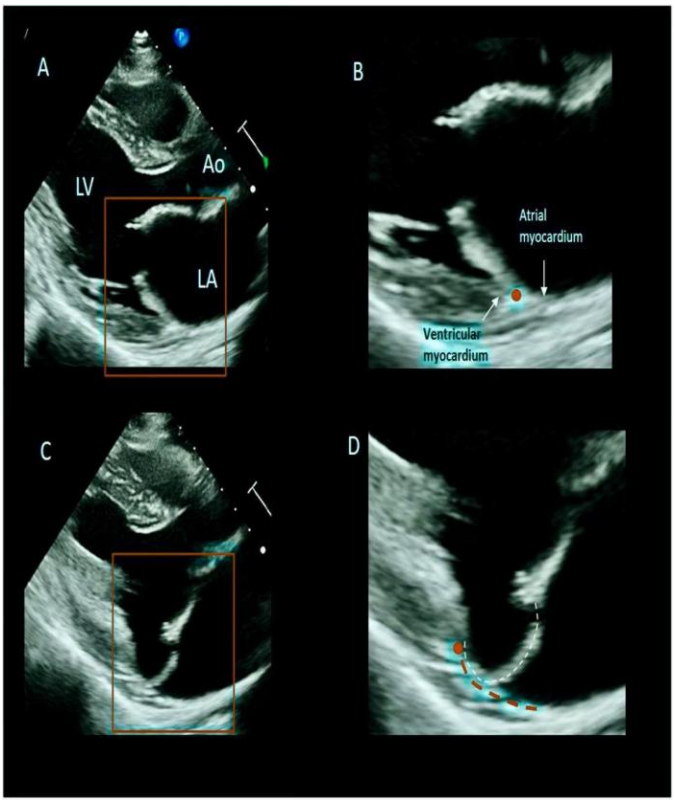

Figure 5: Two-dimensional TTE image in the long-axis view of patients with MVP, in diastole (A) and in systole (C). Panels B and D are magnified images of the structures inside the red squares of panels A and C, respectively. Panel B shows that in diastole the hinge line of the posterior leaflet is correctly attached at the junction of the atrial and ventricular myocardium (red circle). Panel C and D shows that in systole the disjunction is made up by the apposition of leaflet tissue (white dotted line) and atrial wall (red dotted line). AO, Aorta; LA, left atrium.

Despite that MAD could be present in healthy hearts, some authors revealed its connection with the arrhythmic MVP phenotype [9, 11, 12]. MAD leads to the excessive mobility of the leaflets, accounting for a mechanical stretch of the inferobasal wall and papillary muscles, eventually leading to myocardial damage and fibrosis [10] as a possible substrate for VAs [10] (Figure 6).

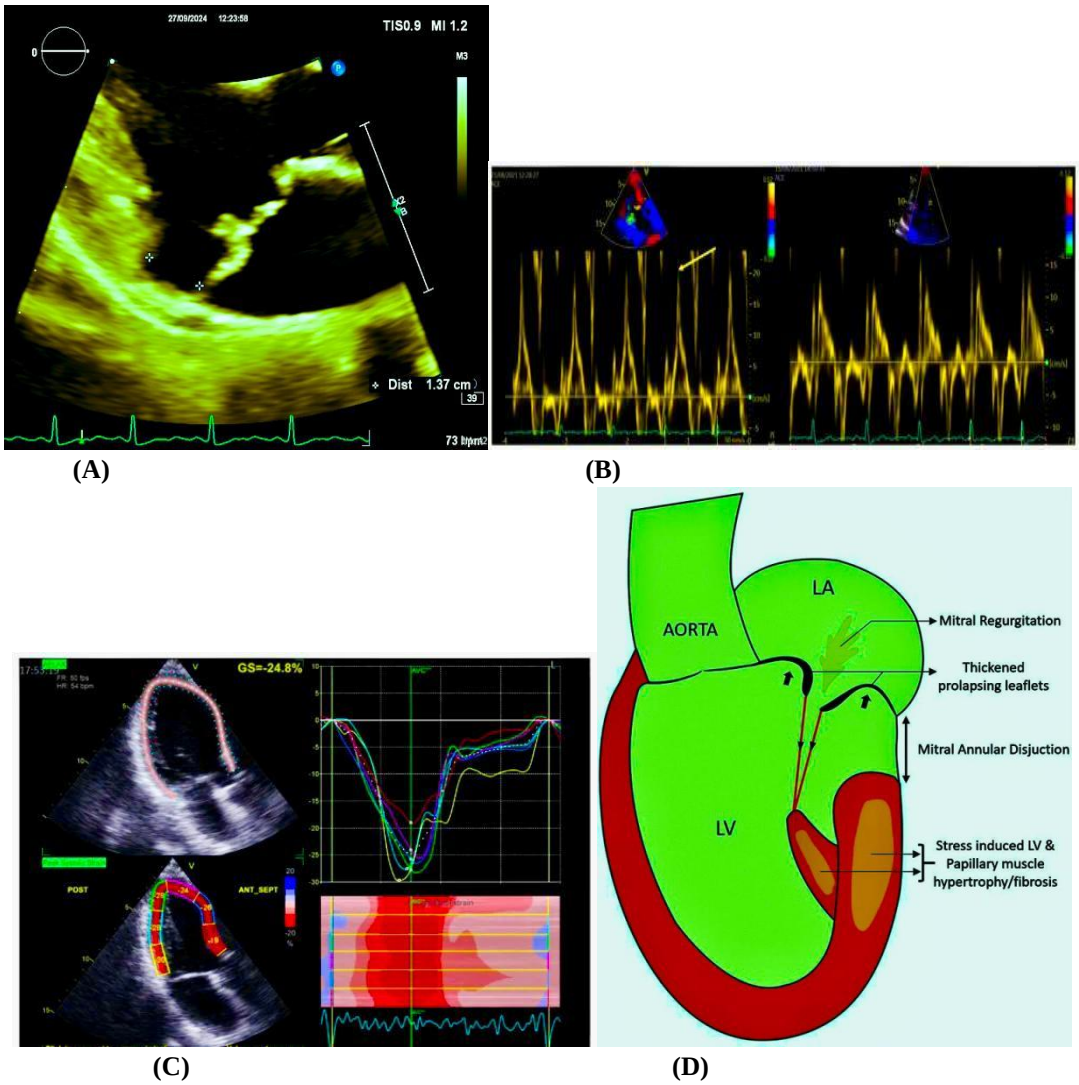

Figure 6: (A) Transthoracic echocardiography (long-axis parasternal view) of MAD measurement. MAD distance is calculated as the length of systolic separation between the left atrial wall and mitral valve leaflet junction to the top of the left ventricle free wall. (B) The presentation of the Pickelhaube sign (yellow arrow) as a spiked configuration of basolateral annular tissue Doppler imaging presentation (left panel). The presentation of S' value of basolateral annular tissue Doppler imaging in patient without Pickelhaube sign (right panel). (C) The example of representative case with speckle-tracking analysis including MAD area. (D) Diagrammatic representation of pathophysiology of MAD and arrhythmic MVP.

Left ventricular strain imaging by speckle tracking echocardiography

Speckle tracking echocardiography (STE) allows a precise measure of myocardial segmental systolic deformation. STE has been shown to reveal subclinical abnormal deformation [13] (Figure 7) and it may offer new insights in the understanding of mitral valve and myocardial interactions in patients of MAD accompanied by MVP [13].

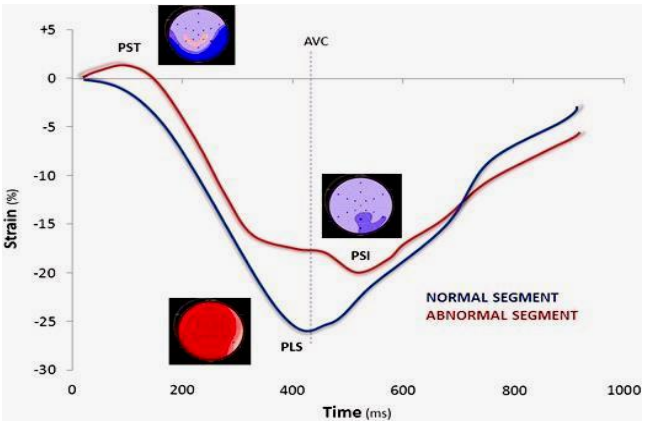

Figure 7: Longitudinal strain curves measured by STE with deformation pattern of a normal segment (blue curve) and an abnormal segment (red curve) with mitral valve leaflet/myocardial interaction. Abnormal segment is

characterized by an early peak with stretch of the segment (PST) with a PSS and peak strain (PSI) therefore occurring beyond AVC. Normal segment presents no or mild PST and PSI with a peak systolic strain (PLS) typically occurring at end-systole.

Changes in longitudinal strain magnitude in MVP

Mitral valve regurgitation is responsible for structural changes in LV and 2DSTE revealed the presence of significant subclinical LV longitudinal dysfunction since the early stages of MR [13]. This analysis of systolic deformation is of clinical interest as a reduction in the absolute value of peak systolic strain (PLS) has been shown to be associated with post-operative LV dysfunction [13].

A recent study analysed the deformation profile in asymptomatic MVP patients and revealed a decrease in the peak longitudinal and peak circumferential strain and strain rate absolute values in septal segments. The authors suggested that these changes may be the first markers of LV remodelling [14].

Case Report

A 54 year adult male presented to our cardiology OPD with the complaints of atypical chest pain and occasional palpitations. The palpitations were for only few seconds. Even though the patient was hypertensive, he was currently, controlled on appropriate medications. The patient denied any history of other cardiovascular risk factors (smoking, tobacco chewing, diabetes, dyslipidemia), thyroid disorders and any episode of syncope.

On clinical examination, the patient was healthy looking and normally built. The patient's weight was 71 kg, height was 158 cm, pulse rate was 86/min, blood pressure was 130/80 mmHg can anti-hypertensive medications, respiratory rate was 16/min and SPO2 was 98% at room air. All the peripheral pulses were normally palpable without any radio-femoral delay.

On cardiovascular examination, there was presence of mid systolic click followed grade 2/4 mid systolic murmur over the LV apex, best heard in the left lateral decubitus position. LV S3 gallop was absent. Rest of the systemic examination was normal.

Xray chest (PA) view and resting ECG were normal (Figure 8).

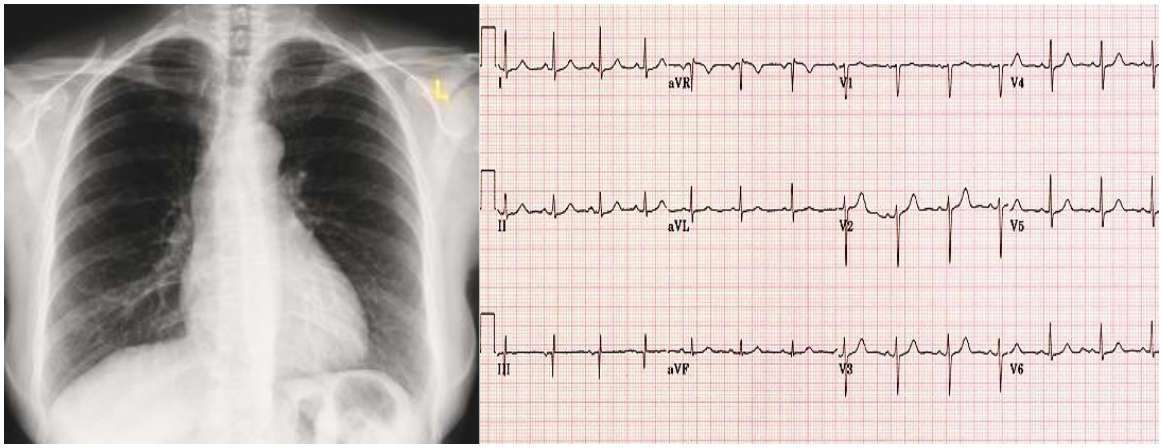

(A) **(B)**

Figure 8: X-ray chest (PA) view normal; (B) Resting ECG normal

Moreover, the pathological investigations for estimation of diabetes, dyslipidemia and thyroid profile were normal.The standard Bruce protocol treadmill stress test and 48 hour holter monitoring to detect the presence of any arrhythmia, were within normal limits.

Transthoracic Echocardiography

All echocardiography evaluations were performed by the author, using My Lab X7 4D XStrain echocardiography machine, Esaote, Italy. The images were acquired using an adult probe equipped with harmonic variable frequency electronic single crystal array transducer while the subject was lying in supine and left lateral decubitus positions.

Conventional M-mode, two-dimensional and pulse wave doppler (PWD) and continuous wave doppler (CWD) echocardiography was performed in the classical subcostal, parasternal long axis (LX), parasternal short axis (SX), 4-Chamber (4CH), 5-Chamber (5CH) and suprasternal views(Figures 9-16).

M-mode Echocardiography

M-mode echocardiography of left ventricle was performed and the estimated measurements are outlined (Table 2, Figure 9).

Table 2:Calculations of M-mode echocardiography

Measurements	LV
IVS d	7.7 mm
LVID d	58.5 mm
LVPW d	6.5 mm
IVS s	13.4 mm
LVID s	34.8 mm
LVPW s	14.2 mm
EF	70 %
% LVFS	41 %
LVEDV	170.1 ml
LVESV	50.2 ml
SV	119.9 ml
LV Mass	153 g

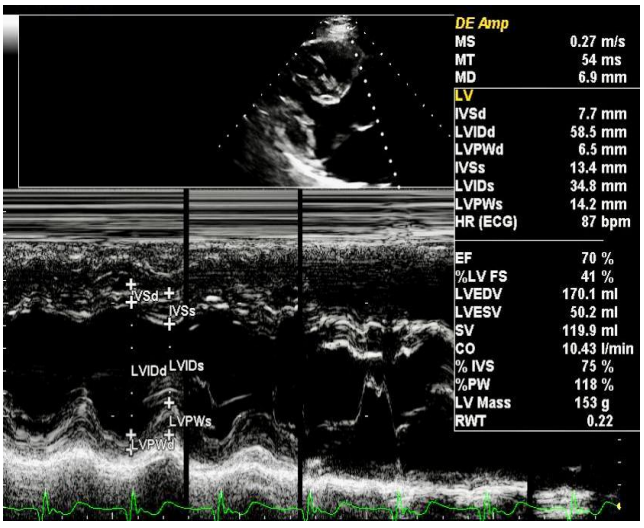

Figure 9: M-mode measurements of left ventricle

Summary of M-mode echocardiography

The LV was dilated with an LV internal dimension in diastole and LVEDV being 58.5 mm and 170.1 ml, respectively. The LVEF was normal -70%.

2Dimensional color echocardiography

Transthoracic color echocardiography exhibited multiple features as outlined below:

- Levocardia
- Situs solitus
- A-V concordance
- V-A concordance
- Concordant D-bulboventricular loop
- Normally related great arteries (NRGA)
- Left aortic arch
- Normal pulmonary and systolic venous drainage

In the LX view, there was conspicuous presence of **mitral valve prolapse of AML and PML.** The superior displacement of AML and PML was 3.7 mm and 4.2 mm, respectively (Figure 10). However, the MV leaflets were thickened and the mitral annulus was dilated (D=35.5 mm). A **significant mitral regurgitation** was demonstrated (Figure 11). MR jet area was 3.69 sqcm, visualized as an eccentrically directed posterior jet. **Mitral annulus disjunction (MAD)** was delineated (Figure 12), and the MAD distance was 9.3 mm.

4Dimensional volumetric data

Table 3 depicts the volumetric data acquired by 4Dimensional XStrain echocardiography

Table 3: 4Dimensional volumetric data

Parameters	Values
LVEDV	80.81 ml
LVESV	29.96 ml
EF	62.93 %
CO	4438.98 ml/min
Sph i d	0.39
Sph i s	0.25

EDV, end diastolic volume; ESV, end systolic volume; EF, ejection fraction; CO, cardiac output; Sph i d, sphericity index diastole; Sph i s, sphericity index systole

AP, apical; 2C, two chamber; LAX, long axis; 4C, four chamber; MV, mitral valve; pap mus, papillary muscle.

Speckle tracking echocardiography

Comprehensive speckle tracking echocardiography (STE) was accomplished by 4Dimensional XStrain technique. The values obtained of various LV strain parameters are enumerated (Table 4):

Table 4: 4Dimensional XStrain echocardiography - estimated values of LV strain parameters in our index patient

LV strain Parameters	Strain (%)	Strain rate (1/s)
Global longitudinal strain (GLS)		
AP 2C	-19.28	1.97
AP LAX	-17.76	1.91
AP 4C	-16.41	1.85
Global strain	-17.81	-
Global circumferential strain (GCS)		
at MV level	-15.04	1.04
at pap mus level	-10.77	1.51
Global radial strain (GRS)		
at MV level	28.78	1.54
at pap mus level	21.94	2.71

Table 5: 4Dimensional XStrain echocardiography estimation of LV segmental endocardial longitudinal strain

Bull's eye analysis		
Endo long strain (Peak)		
Bas Ant	-21.95	%
BasAntSep	-5.69	%
Bas Sep	-12.63	%
Bas Inf	-20.14	%
Bas Post	-41.04	%
Bas lat	-34.88	%
Mid Ant	-27.26	%
MidAntSep	-14.71	%
Mid Sep	-11.03	%
Mid Inf	-15.21	%
Mid Post	-8.95	%
Mid Lat	-15.99	%
Apic Ant	-18.95	%
Apic Sep	-25.34	%
Apic Inf	-18.26	%
Apic lat	-15.93	%
Apex	-16.18	%
Global Strain (A2C)	-19.28	%
Global Strain (ALAX)	-17.76	%
Global Strain (A4C)	-16.41	%
Global Strain	-17.81	%

Red squares depict significant reduction in strain values in multiple segments of LV

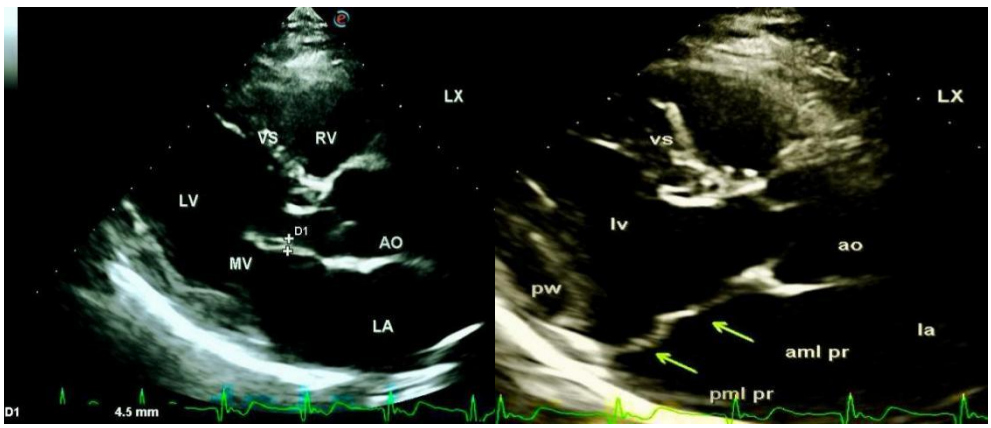

(A) **(B)**

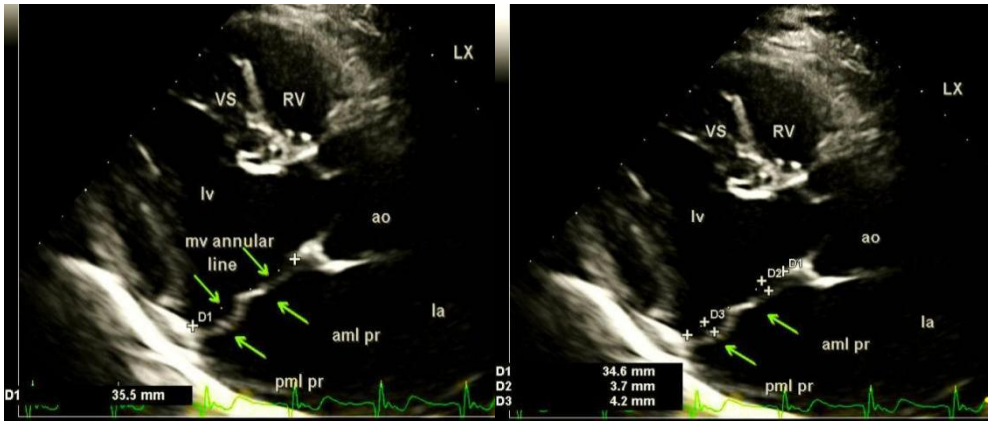

(C) (D)

Figure 10: 2Dimensional transthoracic Echocardiography of mitral valve prolapse. (A) LX view shows thickened mv leaflets; (B) LX depicting superior displacement of AML and PML; (C) LX shows dilatation of mitral valve annulus (D=35.5 mm); (D) LX illustrates the superior displacement of AML and PML from the mitral annular plane of 3.7 mm and 4.2 mm respectively

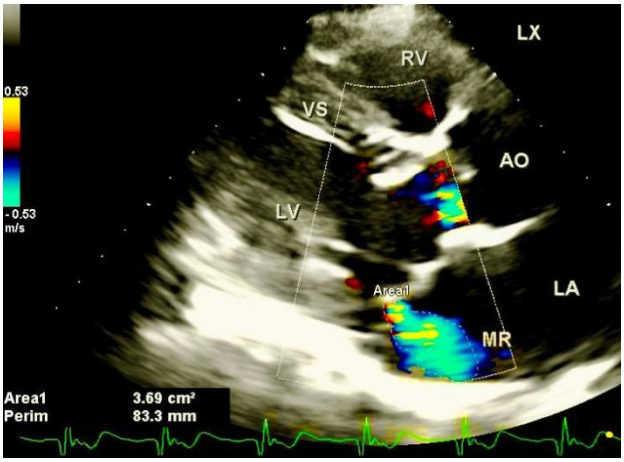

Figure 11: Mitral regurgitation. LX reveals the presence of moderate mitral regurgitation. The area of the jet was 3.69 sqcm.

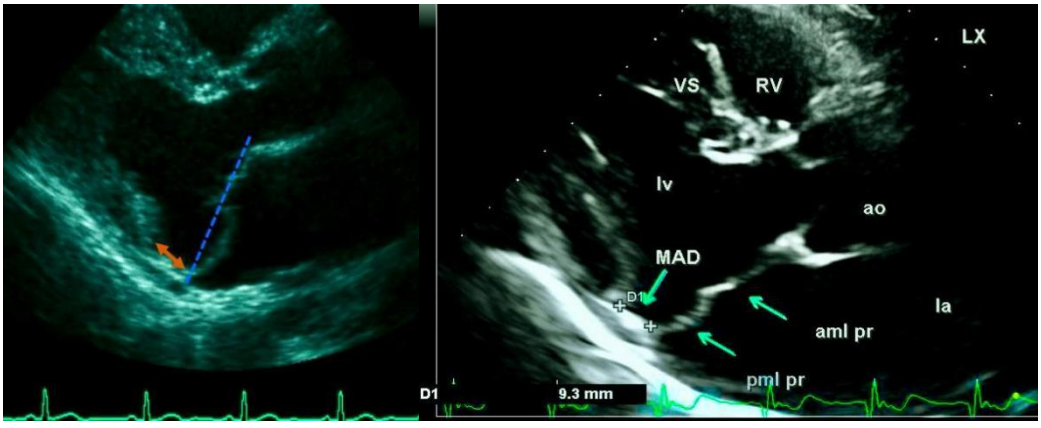

(A) (B)

Figure 12: Mitral annulus disjunction(MAD). (A) 2D echocardiographic illustration of MAD in LX view; (B) MAD in our patient was 9.3 mm

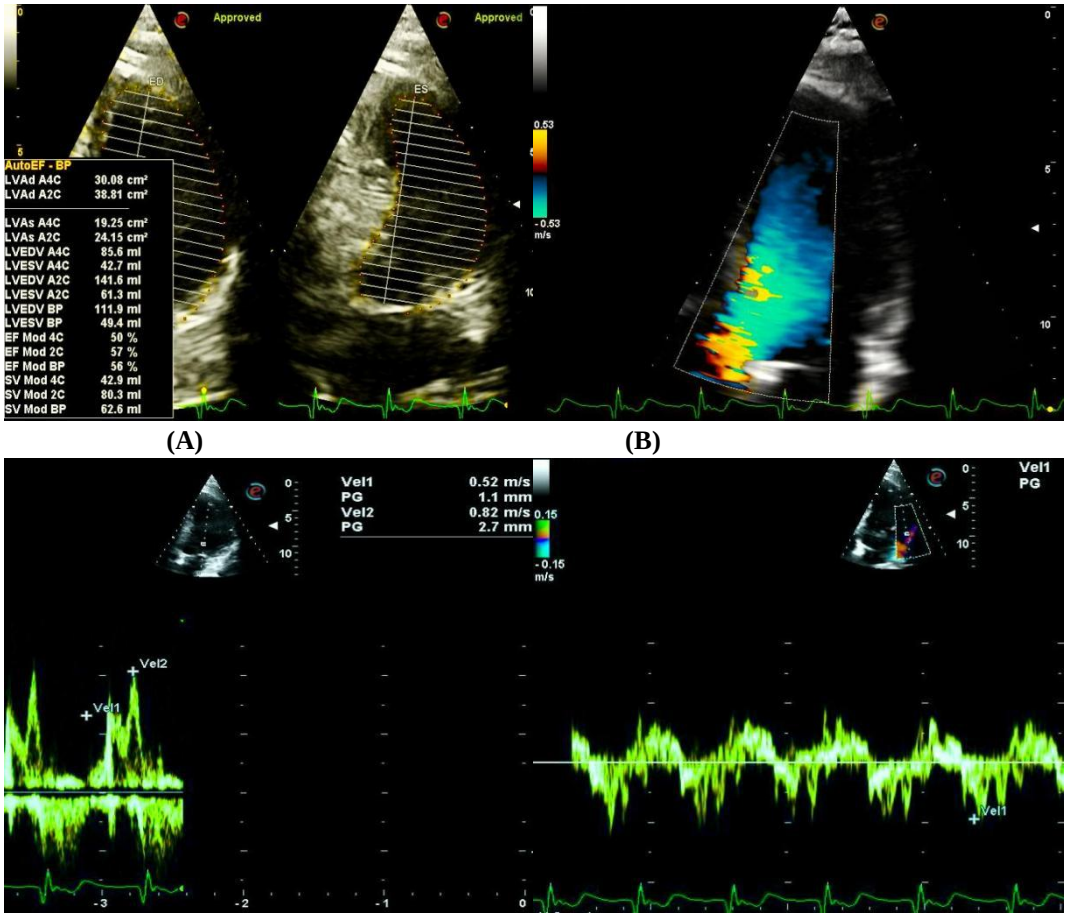

Figure 13: Illustration of LVEF by biplane Simpson's method, absence of LVOT obstruction, pulse wave doppler pattern of mitral velocities and lateral wall LV tissue doppler imaging in our patient. (A) Biplane Simpson's method LVEF was 56 %; (B) Absence of LVOT obstruction in 5C view; (C) Mitral valve velocity reveals LV diastolic relaxation dysfunction grade 1; (D) TDI of lateral wall of LV.

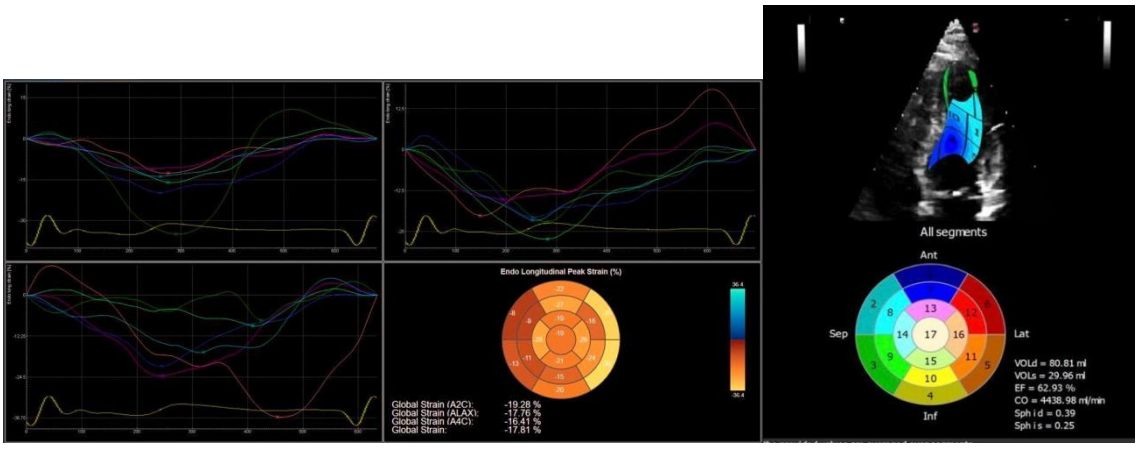

Figure 14: 4Dimensional XStrain speckle tracking echocardiography. (A) Bull's eye plot and graphs of peak endocardial longitudinal strain; (B) 4Dimensional volumetric data derived from XStrain 4D echocardiography.

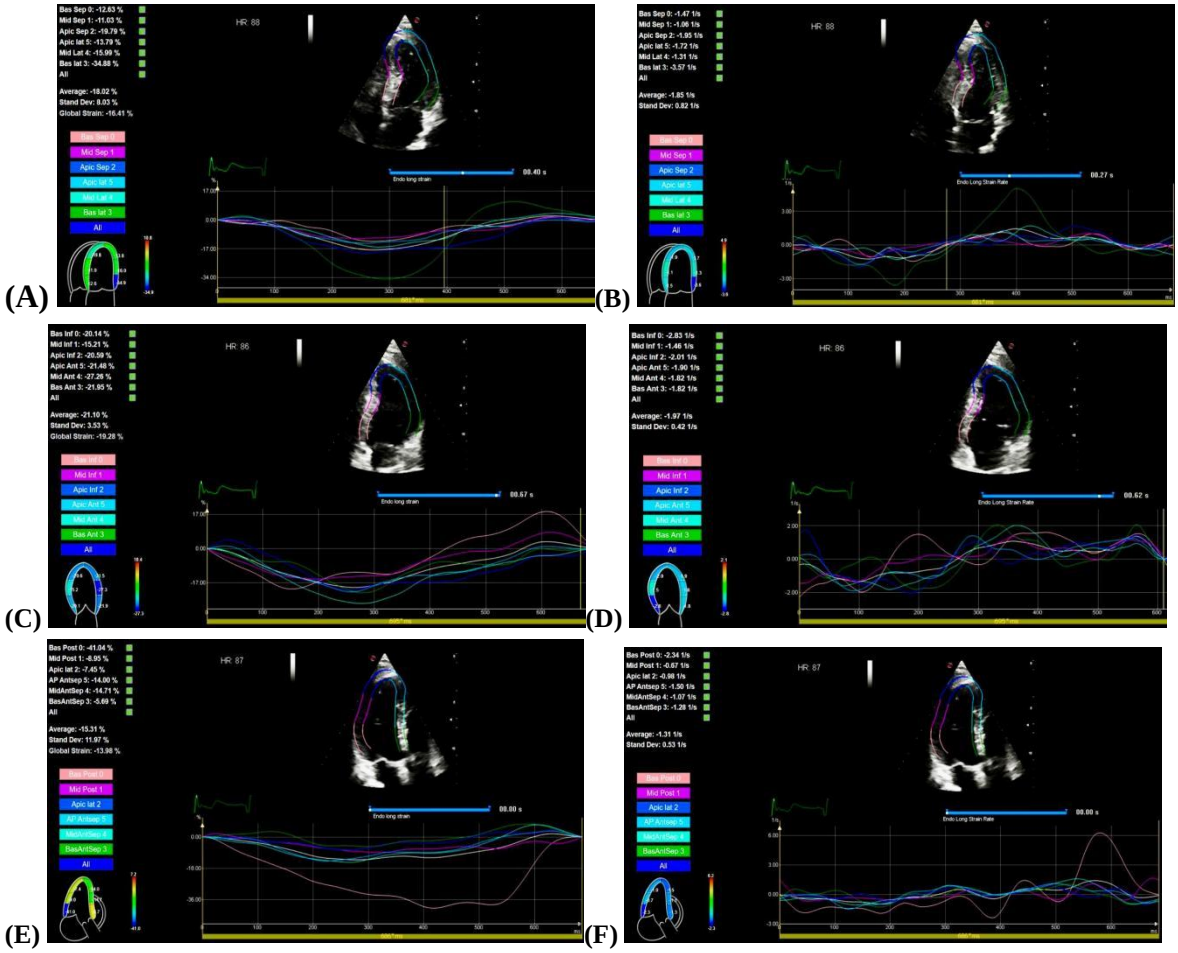

Figure 15: 4Dimensional XStrain Echocardiography. Global longitudinal strain and strain rate of AP4C, AP2C and APLAX views. (A) 4C global longitudinal strain; (B) 4C global longitudinal strain rate; (C) 2C global longitudinal strain; (D) 2C global longitudinal strain rate; (E) LAX, global longitudinal strain; (F) LAX, global longitudinal strain rate; AP, apical; 4C, four chamber; 2C, two chamber; LAX, long axis

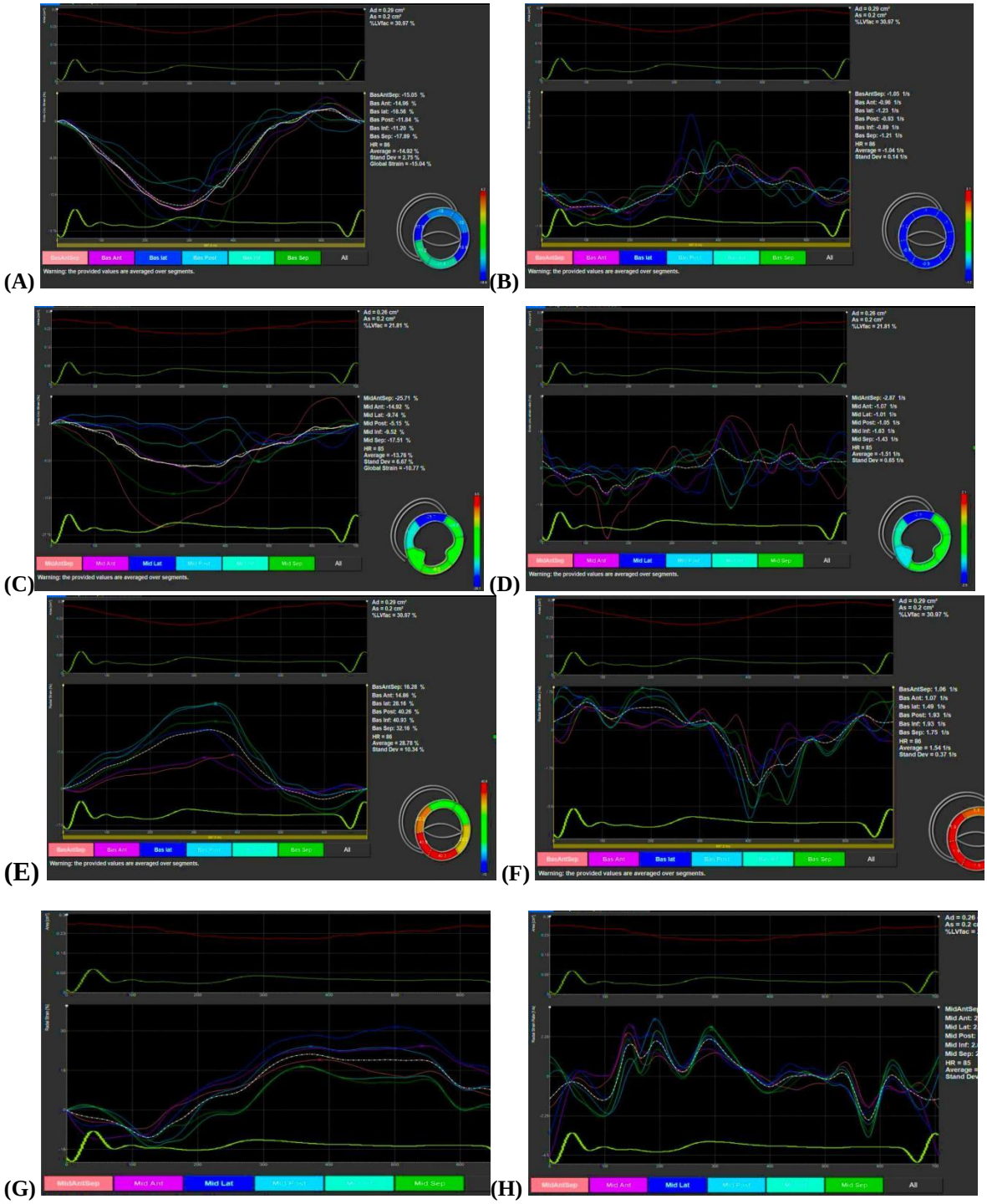

Figure 16: 4Dimensional XStrain Echocardiography. (A) Global circumferential strain, at MV level; (B) Global circumferential strain rate, at MV level; (C) Global circumferential strain, at papillary muscle level; (D) Global circumferential strain rate, at papillary muscle level; (E) Global radial strain, at MV level; (F) Global radial strain rate, at MV level; (G) Global radial strain, at papillary muscle level; (H) Global radial strain rate, at papillary muscle level

Summary of 2Dimensional transthoracic and 4Dimensional XStrain speckle tracking echocardiography

Our index patient, a known hypertensive controlled on anti-hypertensive medications, presented to us with history of atypical chest pain and occasional palpitations. In the backdrop of normal treadmill stress test, holter and various pathological investigation conducted, we performed a comprehensive TTE and 4D XStrain STE with the aim to estimate the mitral annulus disjunction, and moreover, to demonstrate any early features of LV systolic dysfunction by

detecting aberrancy in various LV strain parameters acquired by 4D XStrain STE.

In the standard 2Dimensional TTE we demonstrated primary prolapse of AML and PML, dilatation of mitral valve annulus, moderate grade mitral regurgitation, dilation of LV and MAD distance of 9.3 mm.

On 4D XStrain STE, we illustrated: GLS value of -17.81 %, GCS values at MV and pap mus level of -15.04 % and -10.77 % respectively and GRS values at MV and pap mus level of 28.78 % and 21.94 % respectively. The values of GLS and GCS were lesser than the values of normal 4D STE and 4D XStrain STE, in healthy adults [15, 16]. Furthermore, on segmental LV endocardial longitudinal strain analysis, we delineated significant reduction in strain values in multiple segments (Table 5).

Discussion

The prevalence of MVP is variable. The worldwide prevalence of MVP is between 0.4% and 35% whereas Indian prevalence by echocardiography studies is between 2.7% and 16% [17, 18]. This wide prevalence could be due to the variety of populations studied, both hospital-based and healthy volunteers with a minority still being unrecognized since most are usually asymptomatic. There are very few autopsy studies on MVP with a reported incidence of about 4%-5% at autopsy [19, 20].

MVP is more common in females as compared to males [17]. Myxomatous degeneration is the most common cause of MVP in which there is excessive accumulation of glycosaminoglycan material within leaflets and cusps. Other less common causes include dysfunctional papillary muscles, ruptured chordae tendineae or papillary muscles [21, 22].

Mitral annulus disjunction

Mitral annulus disjunction is an anatomic abnormality involving the confluence of the left atrium, mitral valve annulus, and the base of the left ventricle (Figure 17). It is classically associated with the spectrum of myxomatous disease of the mitral valve and MVP [21, 22].

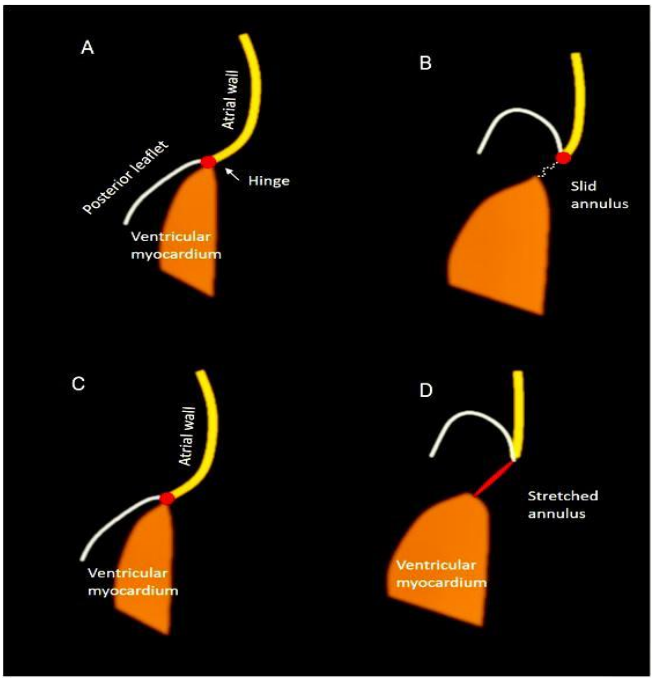

Figure 17: (A, B) First hypothesis on MAD morphology. Although the posterior hinge line is somehow detached by the myocardium, it maintains its own "normal" position. In systole, as the posterior myocardium contracts, the hinge line slides backward, and MAD becomes visible. Which structure/tissue fills the gap between the hinge line and the crest of ventricular myocardium is unclear. (C, D) Second hypothesis: in systole the hinge line is stretched.

History and etymology

The term ‘mitral annular disjunction was first used by Bharati et al. in 1981 and later defined by Hutchins et al. in 1986 [23, 24].

Epidemiology

Mitral annulus disjunction has been reported in 42-90% of patients with myxomatous mitral valve disease and mitral prolapse. The condition seems to be more common in women [1].

Associations

Mitral annular disjunction has been associated with the following clinical conditions [1-4]:

- mitral valve prolapse (MVP)
  - particularly bileaflet prolapse [25]
- myxomatous degeneration of mitral leaflets

- sudden cardiac death
    - ventricular ectopy and dysrhythmias

Classification

A suggested classification for subgrouping MAD by measured degree of disjunction was proposed in 2013 by Konda et al. [26]:

- type I: excessive annular mobility with an absence of a visualized separation between annulus and basal left ventricular myocardium
- type II: annulus-ventricular separation (i.e. disjunction) of less than 5 mm
- type III: disjunction greater than 5 mm

Location

The annulus can be affected throughout its circumference, and may have multiple areas of discontinuous involvement. MAD most commonly occurs at the posterolateral annulus adjacent to the valvular scallops P1 and P2, affecting the posterior leaflet [25]. Involvement of both anterior and posterior leaflets is not uncommonly observed. The least common variant affects the anterior leaflet alone.

The extent of mitral annular disjunction may be quantified by measuring the distance between the insertion of the leaflet at the left atrial wall and the left ventricular myocardium as well as the circumferential extension [1-3] (Figure 18).

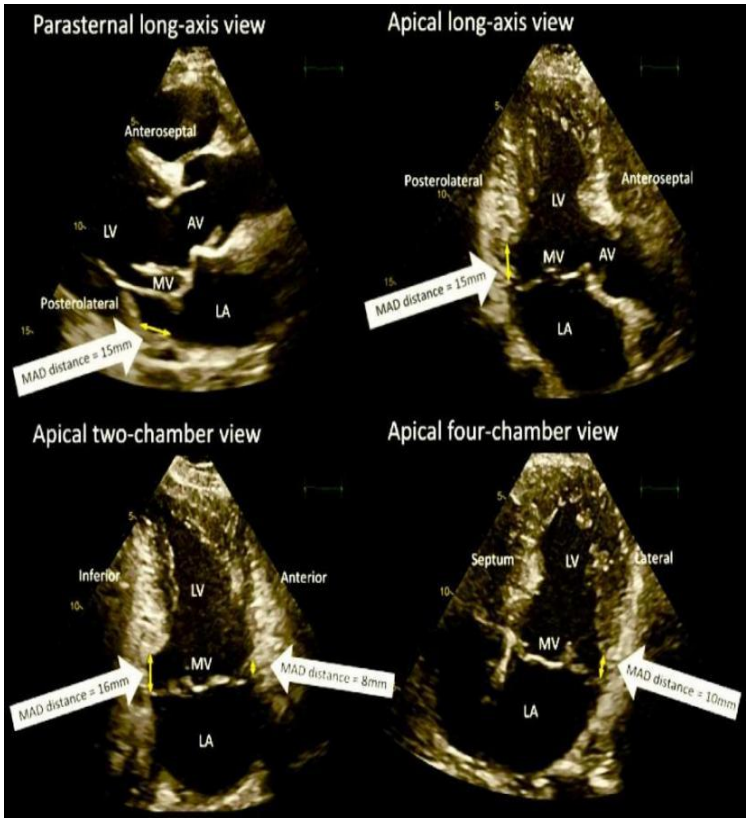

Figure 18: Measurement of Longitudinal MAD Distance in a Transthoracic Echocardiogram. All pictures are at end-systole. Longitudinal MAD distance in the posterolateral wall is measured in parasternal long-axis view. Yellow arrows = longitudinal MAD measurement. AV = aortic valve; LA = left atrium; LV = left ventricle; MAD = mitral annulus disjunction; MV = mitral valve.

Increased severity of MAD has been found to correlate with:

- degree of mitral regurgitation [27]
- number of valve segments with flail or prolapse
- increasing burden of ventricular dysrhythmias

Clinical presentation

Patients may be asymptomatic with an incidental discovery or present with symptomatic dysrhythmias (palpitations, presyncope, dyspnea).

Sudden cardiac death (SCD) is a described presentation.

Physical examination is non-specific, but may reveal findings of related anomalies such as MVP (mid-systolic auscultatory click) or resultant pathologic sequelae such as a displaced point of maximal (apical) impulse with associated left ventricular dilation or a systolic murmur consistent with mitral regurgitation [1, 4].

Radiographic features

Mitral annulus disjunction is most easily appreciable in systole when the detachment of the left inferolateral myocardial wall from the posterolateral portion of the mitral annulus can be demonstrated.

Likewise, the distance between the posterior mitral valvular leaflet insertion at the atrial wall and the connection of the left atrial wall to the myocardial free wall is measured in systole [1-3].

Echocardiography

Echocardiography is considered is usually the first-line imaging modality for the evaluation of mitral valvular disorders [1]. A distance between the posterior mitral leaflet insertion and the left ventricular myocardium of ≥5 mm in transesophageal echocardiography is considered diagnostic [1, 23].

Toh et al [28], in a recent review of 98 subjects with structurally normal hearts, reported that 96% had MAD. No minimum distance was used to define MAD positivity, and the median MAD distance was just 3.0 mm with a range of 1.5 to 7 mm. This is much lower than the average MAD distance noted in many studies involving patients with MVP. Mantegazza et al [29] reported an average MAD distance of 6.6±2.2 mm in surgical patients with MVP and MAD on TTE. Similarly, Essayagh et al [30] found an average MAD distance of 8±4 mm in patients with MVP who were diagnosed with MAD by CMR. Konda et al [31] set a minimum MAD distance of 2 mm by TTE to be considered to have MAD.

Thus, the majority of people, including those with structurally normal hearts, may have some minimal degree of MAD that is more readily identified as the spatial resolution of cardiac imaging improves. The question is then raised of what distance of disjunction represents clinically significant MAD. An early study found that a MAD distance of >8.5 mm by TTE was associated with higher likelihood of NSVT [32]. Perazzolo Marra et al [4] found that MVP patients with LV fibrosis on CMR had a median MAD distance of 4.8 mm, whereas the median MAD distance was only 1.8 mm in MVP patients without LV fibrosis. A more recent study of Lee et al [33] using CMR found an association between the 3-dimensional extent of MAD and mitral regurgitant orifice area. It may be that "pathological" MAD has a more extensive circumferential distribution as well as a greater distance when compared with the MAD seen in normal variants. More research is needed to clarify how the extent of MAD-both maximum distance and circumferential extent-relates to clinical outcomes, to establish a threshold for clinically significant MAD.

In our patient, MAD distance was 9.3, on TTE in the long axis view.

CT

Cardiac CT can identify and depict mitral annulus disjunction as a separation between the left atrial wall mitral valve leaflet junction and left ventricular wall along the mitral annular circumference [23] (Figure 19).

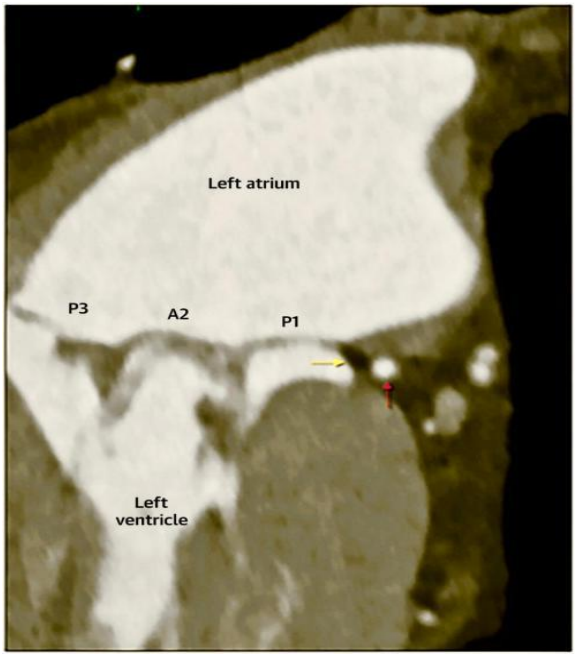

Figure 19: Evaluation of MAD With Computed Tomography. MAD (yellow arrow) seen on computed tomography.

MRI

Cardiac MRI can detect and characterize the circumferential extent of mitral annulus disjunction and systolic curling. The separation distance has been described to vary between 1 and 15 mm [25]. Moreover, cardiac MRI can assess myocardial fibrosis in the basal inferolateral free wall or papillary muscles, which can be depicted with T1 mapping or late gadolinium enhancement [23, 34] (Figure 20).

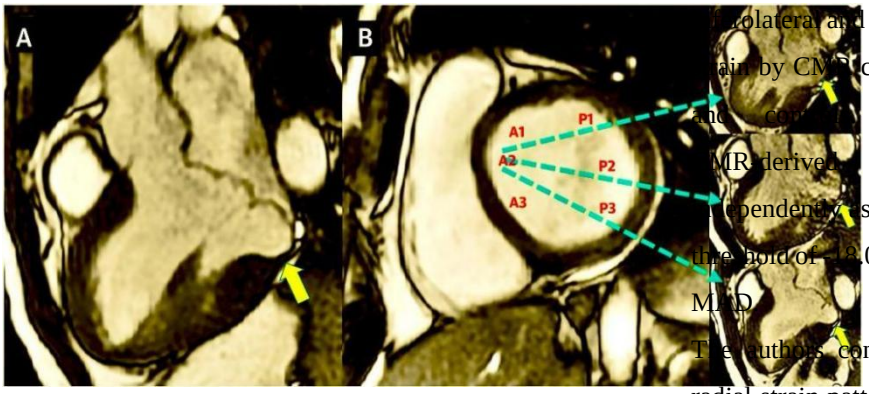

Figure 20: Evaluation of MAD With CMR Imaging. (A) Steady-state free precession, long-axis, 3-chamber view of the left ventricle showing MAD during systole (yellow arrow). (B) Imaging planes proscribed along the direction of the anterior and posterior mitral valve leaflet scallops showing MAD along the entire length of the posterior mitral annulus (yellow arrows). CMR = cardiac magnetic resonance.

CMR has been applied to investigate LV structure and function in patients with MAD [33]. Basal hypertrophy is more common in the lateral and septal walls in patients with MAD vs patients without MAD. The exact mechanism of LV basal hypertrophy in MAD is still unknown, but it may relate to changes in myocardial energetics in response to repetitive traction by MAD and/or MVP [33]. In addition, papillary muscle late gadolinium enhancement (LGE) was more common in those with MAD [33].

Left ventricular strain imaging in MAD

Few studies have investigated the utility of myocardial deformation analysis in MAD [35, 36]. Forty-two patients with MVP (21 with MAD, 21 without MAD) and 21 controls were studied. Global, basal and basal inferolateral segmental strains were measured and compared using velocity-vector imaging TTE and feature-tracking CMR [35].

Patients with MAD and MVP had lower basal longitudinal strain by TTE than those with MVP without MAD. Those with MAD and MVP had lower magnitude in basal inferolateral and basal segments by circumferential and radial strain by CMR compared to those with MVP without MAD and controls. Amongst global strain parameters, CMR derived global circumferential strain was independently associated with MAD diagnosis, with optimal threshold of -18.0% having 76% sensitivity and specificity for MAD.

The authors concluded that abnormal circumferential and radial strain patterns in the basal segments by CMR may be useful for identifying regional LV dysfunction associated with MAD.

Another study aimed to evaluate left ventricular (LV) function using speckle tracking echocardiography in MVP patients with MAD [36]. Transthoracic echocardiography and cardiac magnetic resonance imaging were performed to assess LV function and MAD presence. Late gadolinium enhancement frequency was significantly higher in MAD patients with MVP. MAD patients with MVP had significantly impaired global longitudinal strain, basal longitudinal strain, Mid-Ventricular Longitudinal Strain and LA strain when compared to MVP patients without MAD, despite similar LV ejection fraction. All these values of MVP patients were also significantly lower than the control group. The mean MAD distance was 7.8 ± 3.2 mm in MAD patients with MVP. This study demonstrated a significant decrease in longitudinal strain in MVP patients with MAD, indicating myocardial dysfunction. These findings suggest that MAD may contribute to LV dysfunction and highlight the importance of early detection in younger patients.

In our patient, there was significant alteration in values of GLS, GCS. Moreover, the segmental endocardial longitudinal strain displayed marked reduction in strain values in multiple segments of LV. Normal values of 2Dimensional and 4Dimensional LV strain in healthy subjects is shown in Table 6 and 4Dimensional XStrain STE analysis in healthy adults is outlined in Table 7.

Table 6: 2Dimensional and 4Dimensional LV strain values in healthy subjects [15].

LV parameters	median %	1st - 3rd quartiles
2D Longitudinal strain	-21	-20 to -23
2D Circumferential strain	-22	-20 to -24
2D Radial strain	46	39 to 54
4D Longitudinal strain	-19	-17 to -21

4D Circumferential strain	-18	-17 to -20
4D Radial strain	52	47 to 59

.

Table 7: 4 Dimensional XStrain LV deformation parameters in healthy adults [16].

Apical long axis views	**VARIABLES**	**MALE MEAN + SD**	**FEMALE MEAN + SD**
GLS (%) (-19.10 ±3.12)		-18.99 ± 3.08	-19.41 ± 3.27
2 CH View	GLS (%)	-20.83 ± 4.16	-20.72 ± 3.51
3 CH View	GLS (%)	-17.38 ± 3.17	-18.92 ± 3.42
4 CH View	GLS (%)	-19.12 ± 3.91	18.59 ± 4.97
Short axis views			
mv level	GCS (%)	-16.71 ± 6.55	-15.88 ± 6.01
	GRS (%)	23.11 ± 11.75	18.33 ± 6.70
pap muscle level	GCS (%)	-23.13 ± 6.52	-22.76 ± 7.06
	GRS (%)	25.10 ± 9.93	23.54 ± 11.07

GLS, global longitudinal strain; GCS, global circumferential strain; GRS, global radial strain; mv, mitral valve; pap, papillary; CH, chamber.

Treatment and prognosis

Management apparently differs according to the experience in different centers. Medical therapy with beta-blockers is under consideration [2].

Implantation of an implantable cardioverter-defibrillator (ICD) might be considered as secondary prevention in patients, who have experienced cardiac arrest and no underlying reversible cardiac disease [1, 2].

Conclusion

Mitral annular disjunction is an increasingly recognized entity associated with mitral valve prolapse, ventricular arrhythmias and death. Few studies have investigated the utility of myocardial deformation analysis in MAD. We conducted a comprehensive LV strain imaging by 4Dimensional XStrain STE in an adult male patient afflicted with MVP accompanied by MAD with a significant MAD distance of 9.3 mm.

2Dimensional STE with segmental longitudinal strain may allow for precise evaluation of the myocardium regarding subtle changes. According to the data from the literature, longitudinal strain could be a feasible indicator of future fibrosis appearance in LV segments and 2D STE strain analysis may allow for a more accurate assessment of the arrhythmic risk in MVP patients.

In our index patient, on performing 4D XStrain STE analysis there was a conspicuous reduction of magnitude of GLS, GCS and GRS values and furthermore the longitudinal segmental strain showed striking aberrations in multiple segments of LV. Perhaps, in future, this patient is a potential candidate for serious ventricular arrhythmias, even though he is presently asymptomatic.

REFERENCES

[1] Wunderlich N, Ho S, Flint N, Siegel R. Myxomatous Mitral Valve Disease with Mitral Valve Prolapse and Mitral Annular Disjunction: Clinical and Functional Significance of the Coincidence. J Cardiovasc Dev Dis. 2021;8:9.
[2] Basso C, Iliceto S, Thiene G, Perazzolo Marra M. Mitral Valve Prolapse, Ventricular Arrhythmias, and Sudden Death. Circulation. 2019;140:952-64.
[3] Dejgaard L, Skjølsvik E, Lie Ø et al. The Mitral Annulus Disjunction Arrhythmic Syndrome. J Am Coll Cardiol. 2018;72:1600-9.

[4] Perazzolo Marra M, Basso C, De Lazzari M et al. Morphofunctional Abnormalities of Mitral Annulus and Arrhythmic Mitral Valve Prolapse. Circ Cardiovasc Imaging. 2016;9:e005030.
[5] Freed LA, Levy D, Levine RA, et al. Prevalence and clinical outcome of mitral-valve prolapse. N Engl J Med. 1999;341:1-7.
[6] Parwani P, Avierinos JF, Levine RA, Delling FN. Mitral Valve Prolapse: Multimodality Imaging and Genetic Insights. Prog Cardiovasc Dis. 2017;60:361-369.
[7] Marra MP, Basso C, Lazzari MD, Rizzo S, Cipriani A, Giorgi B, Lacognata C, Rigato I, Migliore F, Pilichou K, et al. Morphofunctional Abnormalities of Mitral Annulus and Arrhythmic Mitral Valve Prolapse. Circ. Cardiovasc. Imaging, 2016;9:e005030.
[8] Carmo P, Andrade MJ, Aguiar C, Rodrigues R, Gouveia R, Silva JA. Mitral annular disjunction in myxomatous mitral valve disease: A relevant abnormality recognizable by transthoracic echocardiography. Cardiovasc. Ultrasound 2010;8:53.
[9] Essayagh B, Sabbag A, Antoine C, Benfari G, Batista R, Yang L-T, Maalouf J, Thapa P, Asirvatham S, Michelena HI, et al. The Mitral Annular Disjunction of Mitral Valve Prolapse: Presentation and Outcome. JACC Cardiovasc. Imaging 2021;14:2073-2087.
[10] Daniłowicz-Szymanowicz L, Zienciuk-Krajka A, Wabich E, Fijałkowski M, Fijałkowska J, Młodziński K and Raczak G. Left Ventricle Segmental Longitudinal Strain and Regional Myocardial Work Index Could Help Determine Mitral Valve Prolapse Patients with Increased Risk of Ventricular Arrhythmias. J. Cardiovasc. Dev. Dis., 2023;10:181.
[11] Sheppard MN, Steriotis AK, Sharma S, Letter by Sheppard et al. Regarding Article, "Arrhythmic Mitral Valve Prolapse and Sudden Cardiac Death". Circulation. 2016;133:e458.
[12] Alenazy A, Eltayeb A, Alotaibi M K, Anwar MK, Mulafikh N, Aladmawi M, Vriz O. Diagnosis of Mitral Valve Prolapse: Much More than Simple Prolapse. Multimodality Approach to Risk Stratification and Therapeutic Management. J. Clin. Med. 2022;11:455.
[13] Huttin O, Pierre S, Venner C, Voilliot D, Sellal JM, Aliot E, Sadoul N, Juillière Y, Selton-Suty C. Interactions between mitral valve and left ventricle analysed by 2D speckle tracking in patients with mitral valve prolapse: one more piece to the puzzle, European Heart Journal - Cardiovascular Imaging. 2017;18:323-331.
[14] Malev EG, Zemtsovskiĭ EV, Omel'chenko MI, Vasina LV. The role of transforming growth factor-ß in the pathogenesis of mitral valve prolapse. Kardiologiia 2012;52:34-9.
[15] Muraru D, Cucchini U, Mihăilă S, Miglioranza MH, Aruta P, Cavalli G, Cecchetto A, Padayattil-Josè S, Peluso D, Iliceto S, . Badano LP. Left Ventricular Myocardial Strain by Three-Dimensional Speckle-Tracking Echocardiography in Healthy Subjects: Reference Values and Analysis of Their Physiologic and Technical Determinants. Journal of the American Society of Echocardiography. 2014;27:858-871.
[16] Mehrotra A, Kacker S , Shadab M, Chandra N, Singh AK. 4 Dimensional XStrain speckle tracking echocardiography: comprehensive evaluation of left ventricular strain and twist parameters in healthy Indian adults during COVID-19 pandemic. Am J Cardiovasc Dis. 2022 15;12:192-204.
[17] Sattur S, Bates S, Movahed MR. Prevalence of mitral valve prolapse and associated valvular regurgitations in healthy teenagers undergoing screening echocardiography Exp Clin Cardiol. 2010;15:e13-5.
[18] Cheng TO. Mitral valve prolapse: The Merchant of Venice or The Tales of Hoffman? European Heart Journal. 2002;23:87-8.
[19] Watanabe C, Sugiura M, Ohkawa S, Ito Y, Toku A, Maeda S, et al Pathology and histochemistry of mitral valve prolapse J Cardiol. 1993;23:69-77.
[20] Anders S, Said S, Schulz F, Püschel K. Mitral valve prolapse syndrome as cause of sudden death in young adults Forensic Sci Int. 2007;171:127-30.
[21] Edwards JESilver MD. Pathology of mitral incompetence Cardiovascular Pathology. 1983 New York, Edinburg Churchill Livingstone:575-98.
[22] Virmani R, Atkinson JB, Forman MB. The pathology of mitral valve prolapse Herz. 1988;13:215-26.
[23] Bharati S, Granston A, Liebson P, Loeb H, Rosen K, Lev M. The Conduction System in Mitral Valve Prolapse Syndrome with Sudden Death. Am Heart J. 1981;101:667-70.
[24] Hutchins G, Moore G, Skoog D. The Association of Floppy Mitral Valve with Disjunction of the Mitral Annulus Fibrosus. N Engl J Med. 1986;314:535-40.
[25] Eriksson M, Bitkover C, Omran A et al. Mitral Annular Disjunction in Advanced Myxomatous Mitral Valve Disease: Echocardiographic Detection and Surgical Correction. J Am Soc Echocardiogr. 2005;18:1014-22
[26] Konda T, Tani T, Furukawa Y. Mitral Annular Disjunction in Consecutive Cases: Echocardiographic Detection. J Am Coll Cardiol. 2013;61:E1046.
[27] Muthukumar L, Rahman F, Jan M et al. The Pickelhaube Sign: Novel Echocardiographic Risk Marker for Malignant Mitral Valve Prolapse Syndrome. JACC Cardiovasc Imaging. 2017;10:1078-80.
[28] Toh H, Mori S, Izawa Y, Fujita H, Miwa K, Suzuki M, Takahashi Y, Toba T, Watanabe Y, Kono AK, et al. Prevalence and extent of mitral annular disjunction in structurally normal hearts: comprehensive 3D analysis using cardiac computed tomography. Eur Heart J Cardiovasc Imaging. 2021;22:614-622.
[29] Mantegazza V, Volpato V, Gripari P, Ghulam Ali S, Fusini L, Italiano G, Muratori M, Pontone G, Tamborini G, Pepi M. Multimodality imaging assessment of mitral annular disjunction in mitral valve prolapse. Heart. 2021;107:25-32.
[30] Essayagh B, lacuzio L, Civaia F, Avierinos JF, Tribouilloy C, Levy F. Usefulness of 3-tesla cardiac magnetic resonance to detect mitral annular disjunction in patients with mitral valve prolapse. Am J Cardiol. 2019;124:1725-1730.
[31] Konda T, Tani T, Suganuma N, Fujii Y, Ota M, Kitai T, Kaji S, Furukawa Y. Mitral annular disjunction in patients with primary severe mitral regurgitation and mitral valve prolapse. Echocardiography. 2020:37:1716-1722.
[32] Carmo P, Andrade MJ, Aguiar C, Rodrigues R, Gouveia R, Silva JA. Mitralannular disjunction in myxomatous mitral valve disease: a relevant abnormality recognizable by transthoracic echocardiography. Cardiovasc Ultrasound. 2010:8:53.
[33] Lee AP, Jin CN, Fan Y, Wong RHL, Underwood MJ, Wan S. Functional implication of mitral annular disjunction in mitral valve prolapse: a quantitative dynamic 3D echocardiographic study. JACC Cardiovasc Imaging. 2017:10:1424-1433.
[34] Zhou N, Zhao Q, Zeng X, Zheng D, Yue J, Zhang K, Mao D, Makielski JC, Cheng J. Association of mitral annular disjunction with premature cardiac mortality in a large series of autopsies. J Am Coll Cardiol. 2021;77:102- 104.
[35] Wang TKM, Kwon DH, Abou-Hassan O, Chetrit M, Harb SC, Patel D, Kalahasti V, Popovic ZB, Griffin BP, Ayoub C. Strain evaluation for mitral annular disjunction by echocardiography and magnetic resonance imaging: a case-control study. International Journal of Cardiology. 2021;334:154-156.
[36] Özyıldırım S, Guven B, Yumuk MT, Barman HA, Dogan O, Topel C, Atici A, Donmez A, Kucukoglu MS, Dogan SM. Evaluation of left ventricular function in patients with mitral annular disjunction using speckle tracking echocardiography. Echocardiograyphy. 2024;41:e15813.